Journal of Medicinal Chemistry

Freie Universität Berlin

Brief Article

Differential targeting of human topoisomerase II isoforms with small molecules

Angelica Mariani, Alexandra Bartoli, Mandeep Atwal, Ka C. Lee, Caroline A. Austin, and Raphaël Rodriguez

J. Med. Chem., **Just Accepted Manuscript** • Publication Date (Web): 06 May 2015

Just Accepted

ACS Publications
High quality. High impact.

Journal of Medicinal Chemistry is published by the American Chemical Society. 1155 Sixteenth Street N.W., Washington, DC 20036

Differential targeting of human topoisomerase II isoforms with small molecules

Angelica Mariani[1], Alexandra Bartoli[1], Mandeep Atwal[2], Ka C. Lee[2], Caroline A. Austin[2,*], and Raphaël Rodriguez[1,3,*]

[1]Centre de Recherche de Gif, Institut de Chimie des Substances Naturelles du CNRS, Avenue de la Terrasse, 91198 Gif-sur-Yvette, France. [2]Institute for Cellular and Molecular Biosciences, Newcastle University, Newcastle upon Tyne, NE2 4HH, United Kingdom. [3]Institut Curie Research Centre, Organic Synthesis and Cell Biology Group, 26 rue d'Ulm, 75248 Paris Cedex 05, France.

ABSTRACT: The TOP2 poison etoposide has been implicated in the generation of secondary malignancies during cancer treatment. Structural similarities between TOP2 isoforms challenge the rational design of isoform-specific poisons to further delineate these processes. Herein, we describe the synthesis and biological evaluation of a focused library of etoposide analogues, with the identification of two novel small molecules exhibiting TOP2B-dependent toxicity. Our findings pave the way towards studying isoform-specific cellular processes by means of small molecule intervention.

INTRODUCTION

Small molecules can interfere with DNA-templated processes with valuable spatiotemporal resolution, providing the means to trigger and modulate disease-relevant mechanisms.[1] TOP2 are nuclear enzymes required to unfold and release DNA topological strain through the cleavage, strand passage and re-ligation of double-stranded DNA.[2] This molecular event involves the formation of reversible enzyme-DNA covalent complexes, representing an intrinsic threat that can lead to cell death. Clinically approved anti-neoplastic agents that target TOP2 operate by stabilizing the normally transient covalent protein-DNA complexes, thereby preventing re-ligation.[3] The proteolytic degradation of such complexes reveals DNA double-strand breaks (DSBs), which in turn activate the DNA-damage response (DDR) machinery to repair DNA lesions.[4] Unrepaired DSBs can either trigger cell death or, alternatively promote genome rearrangements associated with therapy related leukemia.[5] Etoposide (VP-16)[6] targets both TOP2 isoforms in mammalian cells.[7] The α isoform (TOP2A) is required for replication,[8] whereas both isoforms are involved in transcription.[9] Recent findings implicate TOP2B in VP-16-induced DNA-breaks and carcinogenesis, whereas the desired toxicity against cancer cells has been proposed to rely on the targeting of TOP2A.[5,10] While isoform-selective TOP2 poisons can provide valuable mechanistic insights,[5b,11] the structural homology between TOP2 isoforms has so far challenged the development of potent isoform-specific VP-16-derived drugs. The high-resolution crystal structure of a ternary VP-16-TOP2B catalytic core-DNA complex has revealed unprecedented information on the binding mode of VP-16.[12] Remarkably, the glycosidic moiety of VP-16 is in close spatial proximity to a polar glutamine residue (Q778) of TOP2B, a position that is occupied by an apolar methionine (M762) in TOP2A. Hence, we sought to take advantage of this structural variation to explore the ability of synthetic analogues of VP-16 to differentially poison either isoform in human cancer cells. Interestingly, TOP2B778Q and TOP2A762M align with residue serine 83 in gyrase A, a bacterial type II topoisomerase and it has been shown that mutations in serine 83 confer resistance to 4-quinolone antibiotics. This finding functionally demonstrates that a single residue alteration in the active site can alter drug targeting, thus lending strong support to our approach.[13]

Scheme 1. Synthetic strategy and molecular structures of VP-16 analogues.

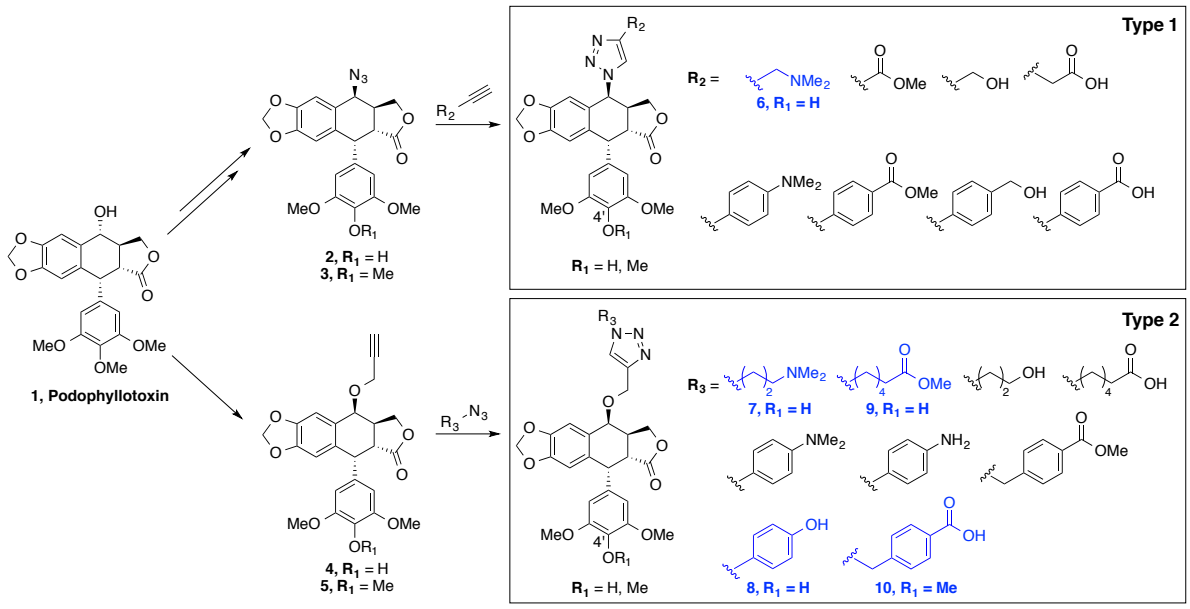

RESULTS AND DISCUSSION

A library of 34 small molecules was prepared based on the main scaffold of VP-16 (**Scheme 1**). Each analogue consisted of the replacement of the sugar moiety with a triazole-containing fragment conveniently introduced by means of thermal or copper catalyzed alkyne-azide cycloadditions (Supporting Information). We explored various linker length, steric hindrance and polarity. Analogues could be categorized in two main classes based on the nature of the triazole orientation (**Type 1** vs **Type 2**, **Scheme 1**), comprising polar substituents expected to be either positively or negatively charged at physiological pH, H-bond acceptor/donor as well as aromatic and aliphatic fragments. Additionally, this focused library contained both 4'-demethyl and -methylated counterparts to further explore the effect of this substitution on the TOP2 isoform-specific targeting capacity of the small molecules.

To assess the ability of each analogue to poison TOP2 *in cellulo*, we performed a "trapped in agarose DNA immunostaining" (TARDIS) assay, which allows for the quantification of drug-stabilized TOP2-DNA complexes using isoform-specific immunofluorescence detection.[14] The library was first screened in a single-dose experiment in K562 human leukemia cells, known to express similar levels of both isoforms (**Table S1- S2**, Supporting Information).[15] From this initial screen, we identified compounds **6**, **7**, **8** and **9** (**Scheme 1**) as TOP2 poisons, which were subsequently investigated in more detail including dose-response treatments (**Figure 1A/B** and **Figure S1-S6**, Supporting Information). We found that analogues harboring an aliphatic spacer and/or a type 2 triazole-linker exhibited a wide range of activity, presumably due to a high degree of rotational freedom enabling stabilizing interactions within the binding pocket of TOP2. While each active small molecule targeted both isoforms, our analysis revealed that **6** exhibited a detectable preference for TOP2B over TOP2A compared to VP-16. The introduction of a 4'-methoxy substituent completely abolished the activity of the small molecules, perhaps reflecting the ability of the 4'-OH to interact with a key residue of TOP2B.[12] Moreover, negatively charged derivatives where inactive, in line with the poor capacity of such functional groups to operate near nucleic acids due to electrostatic repulsion with the DNA phosphate backbone. Hence, compound **10** (**Scheme 1**), which contains both a 4'-methoxy substitution and a negatively charged group, was used as a negative control in subsequent experiments.

These results prompted us to investigate whether the trapping of TOP2-DNA covalent complexes led to the production of DSBs. Thus, we monitored the occurrence of a surrogate mark of DSBs, the phosphorylation of histone protein H2A, X variant on Ser139 (termed γ–H2AX), one of the earliest cellular events in response to DNA damage.[16] To do so, we independently treated K562 cells with 100 μM of each analogue and monitored γ–H2AX by means of immunofluorescence (**Figure 1A/C** and **Figure S6**, Supporting Information). Consistent with the TARDIS data, the small molecules that poisoned TOP2 triggered the production of γ-H2AX characteristic of the DDR, with the general trend of **6** > **8** > **9** > **10**. In contrast to the TARDIS data, we observed that compound **7** displayed a superior ability to generate DSBs compared to the other synthetic analogues that was comparable to VP-16, whilst exhibiting a similar TOP2 targeting capacity compared to **6**. Since the activation of the DDR requires the enzymatic processing of the TOP2-DNA-drug complexes,[4] this result suggested that ternary complexes formed with **7** may be detected and processed differently than complexes formed with the other analogues. It is conceivable that a more favorable kinetics of ternary complex formation with **7** led to a faster proteolytic processing and a higher rate of DSBs mark production. However we cannot rule out that com-

pound **7** exerts its activity partly as a result of a TOP2-independent mechanism.

We next investigated the contribution of each isoform to the inhibition of Nalm-6 leukemia cell proliferation upon treatment with VP-16 analogues. While TOP2B double knockout cells are viable, TOP2A is essential for cell survival. Thus, we employed Nalm-6$^{TOP2A+/-}$ expressing ~50% of TOP2A compared to wild-type (WT) and Nalm-6$^{TOP2B-/-}$ lacking TOP2B.[5b,11]

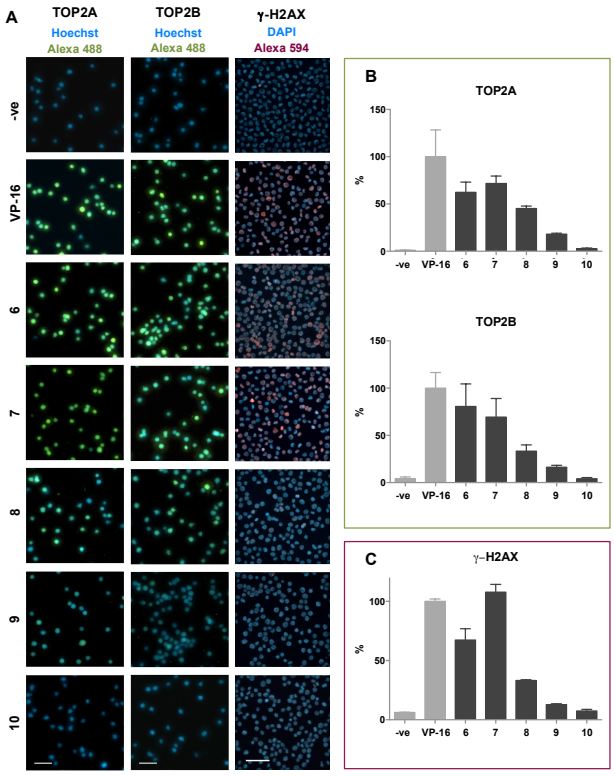

Figure 1. A) Microscope images showing the nucleus (blue), trapped TOP2 (green) and γ-H2AX (red). B) Quantification of fluorescence in the TARDIS assay normalized against VP-16-treated cells. C) Quantification of fluorescence in γ-H2AX positive cells normalized against VP-16-treated cells. Cells were treated with 100 μM VP-16, **6**, **7**, **8**, **9**, **10** or DMSO (-ve). Scale bars, 100 μm.

We found that compounds **6** and **7** were the most potent analogues of the series with IC_{50} values of 0.62 μM and 1.2 μM against WT cells (**Table 1**), respectively, consistent with the data obtained from TARDIS and γ–H2AX assays. Interestingly, Nalm-6$^{TOP2B-/-}$ cells were less susceptible to growth inhibition by **6** and **7** than WT and Nalm-6$^{TOP2A+/-}$ cells, with IC_{50} values of 1.32 μM and 2.36 μM, respectively. In contrast, VP-16 was more potent against the Nalm-6$^{TOP2B-/-}$ compared to Nalm-6$^{TOP2A+/-}$ cells. Altogether, these results indicated that cell death inducted by **6** and **7** involved TOP2B targeting to a greater extent than for growth inhibition by VP-16. It is noteworthy that **6** and **7**, which contain positively charged substituents, displayed a higher potency compared to the other analogues, consistent with the ability of such functionalities to engage electrostatic interactions with polar amino acid residues such as the one found at residue 778 of TOP2B. As anticipated, the neutral (**9**) and negatively charged (**10**) analogues, which induced low levels of γ–H2AX, exhibited little antiproliferative properties against the cell lines studied. Strikingly, we found that compound **8** exhibited almost identical IC_{50} values against WT and Nalm-6$^{TOP2A+/-}$ cells (~3.4/3.5 μM), while it was significantly more potent against Nalm-6$^{TOP2B-/-}$ cells with an IC_{50} value of 1.92 μM. This atypical profile suggested a more complex mechanism of action for compound **8** compared to the other analogues.

Table 1. IC_{50} values and selectivity against TOP2A and TOP2B

	IC_{50} (μM)			IC_{50} ratio	
	WT	*TOP2A+/-*	*TOP2B-/-*	*TOP2A+/-* /WT	*TOP2B-/-* /WT
VP-16	0.134 ± 0.007	0.234 ± 0.003	0.182 ± 0.004	1.7	1.4
6	0.62 ± 0.01	0.85 ± 0.02	1.32 ± 0.01	1.4	2.1
7	1.2 ± 0.1	1.90 ± 0.08	2.36 ± 0.07	1.6	2.0
8	3.4 ± 0.2	3.5 ± 0.1	1.92 ± 0.07	1.0	0.6
9	3.90 ± 0.06	N.D.	N.D.	N.D.	N.D.
10	> 10	N.D.	N.D.	N.D.	N.D.

Cell lines: Nalm-6 (WT), Nalm-6$^{TOP2A+/-}$ (*TOP2A*+/-) and Nalm-6$^{TOP2B-/-}$ (*TOP2B*-/-). Data are means ±SD from 3 replicate experiments. N.D, not determined.

CONCLUSIONS

In conclusion, we have described a series of VP-16 analogues where the sugar moiety was strategically replaced by chemically diverse substituents. Our data demonstrates that structural reprogramming of the scaffold of VP-16 enables the fine-tuning of TOP2 isoform-specific targeting in K562 and Nalm-6 human leukemia cells, thereby providing proof-of-principle for the development of isoform-specific TOP2 drugs derived from VP-16. For instance, we have found that positively charged substrates such as **6** and **7** showed a propensity to affect cell viability in a manner that was reliant on TOP2B to a greater extent than VP-16, thus enabling the study of TOP2B-mediated genomic processes. Additional structural investigations are certainly required to interrogate the very nature of chemical interactions involved between small molecules and TOP2 isoforms with atomic resolution.[12] Since the introduction of a triazole ring was not found to be detrimental to the activity of the most potent derivatives, a future aim is to employ unbiased methodologies such as *in situ* click chemistry and dynamic combinatorial processes to select suitable fragments catalyzed by a specific TOP2 isoform and

identify small molecules with enhanced potency and selectivity.[17]

EXPERIMENTAL SECTION

Chemistry

Podophyllotoxin (**1**) was purchased from Santa Cruz Biotechnology and used without further purifications. 4β-azido-4-deoxy-4'-demethylepipodophyllotoxin (**2**) and 4β-azido-4-deoxyepipodophyllotoxin (**3**) were synthetised as previously described.[18] NMR spectroscopy was performed on Bruker 600 MHz, 500 MHz and 300 MHz apparatus. High-resolution mass spectrometry analysis (HRMS) was performed on a Waters LCT Premier XE, under electron spray ionization (ESI). For final compounds the purity was determined by HPLC (Waters, Alliance 2695, PDA 996 and MS detector) to be >95%.

Synthesis of 4β-(prop-2-ynyloxy)-4'-demethyl-epipodophyllotoxin (4). Podophyllotoxin (**1**, 0.47 g, 1.13 mmol, 1 equiv) was dissolved in dry DCM (11 ml). Sodium iodide (0.51 g, 3.40 mmol, 3 equiv) was added and the resulting suspension was stirred at RT for 5 min. Methanesulfonic acid (220 μl, 3.40 mmol, 3 equiv) was added dropwise at 0°C and the mixture was then warmed to rt and stirred overnight. The solvent was removed under vacuum and the crude product was resuspended in dry THF (10 ml). $BaCO_3$ (223 mg, 1.13 mmol, 1 equiv) and propargyl alcohol (10 ml, 173 mmol, 153 equiv) were added and the mixture was additionally stirred for 3 h at rt. The reaction was quenched with a 10% $Na_2S_2O_3$ aqueous solution and diluted with H_2O. The product was extracted with ethyl acetate and the collected organic phases were dried over $MgSO_4$. The crude product was purified by flash chromatography (DCM: ethyl acetate = 8:2). Compound **4** was obtained as a white solid (245 mg, 0.56 mmol, 49%). ^{1}H NMR (500 MHz, $CDCl_3$) δ 6.94 (1H, *s*), 6.56 (1H, *s*), 6.26 (2H, *s*), 6.00 (1H, *s*), 5.96 (1H, *s*), 5.40 (1H, *s*), 4.79 (1H, *d*, *J* = 2.0 Hz), 4.60 (1H, *d*, *J* = 4.5 Hz), 4.39-4.31 (2H, *m*), 4.27 (2H, *s*), 3.76 (6H, *s*), 3.37 (1H, *dd*, *J* = 4.5, 14.0 Hz), 2.93-2.87 (1H, *m*), 2.57 (1H, *s*). ^{13}C NMR (125 MHz, $CDCl_3$) δ 174.9, 148.5, 146.8, 146.4, 134.0, 132.9, 130.8, 128.3, 111.0, 109.5, 107.9, 101.5, 79.5, 75.6, 71.9, 67.4, 56.4, 56.3, 43.8, 41.0, 37.9. HRMS (ESI) *m/z* calcd for $C_{24}H_{23}O_8$ $[M+H]^+$: 439.1387, found: 439.1377.

Synthesis of 4β-(prop-2-ynyloxy) epipodo-phyllotoxin (5). Podophyllotoxin (**1**, 0.46 g, 1.11 mmol, 1 equiv) was dissolved in dry acetonitrile (11 ml). Sodium iodide (333 mg, 2.22 mmol, 2 equiv) was added and the resulting suspension was stirred at RT for 5 min. Methanesulfonic acid (144 ml, 2.22 mmol, 2 equiv) was added dropwise at 0°C and the mixture was then warmed to rt and stirred for 15 min. The solvent was removed under vacuum and the crude product was resuspended in dry THF (10 ml). $BaCO_3$ (219 mg, 1.11 mmol, 1 equiv) and propargyl alcohol (10 ml, 173 mmol, 156 equiv) were added and the mixture was additionally stirred for 30 min at rt. The reaction was quenched with a 10% $Na_2S_2O_3$ aqueous solution and diluted with H_2O. The product was extracted with ethyl acetate and the collected organic phases were dried over $MgSO_4$. The crude product was purified by flash chromatography (DCM: ethyl acetate = 9:1). Compound **5** was obtained as a white solid (309 mg, 0.68 mmol, 62%). ^{1}H NMR (500 MHz, $CDCl_3$) d 6.94 (1H, *s*), 6.56 (1H, *s*), 6.25 (2H, *s*), 6.00 (1H, *d*, *J* = 1.0 Hz), 5.97 (1H, *d*, *J* = 1.0 Hz), 4.79 (1H, *d*, *J* = 3.0 Hz), 4.61 (1H, *d*, *J* = 5.0 Hz), 4.40-4.33 (2H, *m*), 4.27 (2H, *d*, *J* = 2.5 Hz), 3.80 (3H, *s*), 3.74 (6H, *s*), 3.38 (1H, *dd*, *J* = 5.0, 13.5 Hz), 2.95-2.88 (1H, *m*), 2.56 (1H, *t*, *J* = 2.5 Hz). ^{13}C NMR (125 MHz, CDCl) δ 174.8, 152.6, 148.6, 146.9, 137.3, 135.4, 132.8, 128.3, 111.0, 109.6, 108.3, 101.5, 79.5, 75.6, 71.9, 67.5, 60.8, 56.32, 56.29, 44.0, 41.0, 38.0. HRMS (ESI) *m/z* calcd for $C_{25}H_{25}O_8$ $[M+H]^+$: 453.1544, found: 453.1588.

General procedure for the synthesis of type 1 compounds. 4β-azido-4-deoxy-4'-demethylepipodophyllotoxin (**2**) or 4β-azido-4-deoxyepipodophyllotoxin (**3**) (1 equiv) was suspended in a water: *t*-butanol mixture (1:1) and degassed for 5 min with argon. The appropriate alkyne (10 equiv) was added followed, in order, by sodium ascorbate and $CuSO_4$•$5H_2O$.The mixture was stirred at 50°C till completion. The final suspension was diluted with H_2O and extracted with ethyl acetate. The collected organic phases were dried over $MgSO_4$ and the solvent was removed under reduced pressure. The mixture was purified by flash chromatography or by HPLC.

4β-(4-*N,N*-dimethylaminomethyl-1,2,3-triazolyl)-4'-demethylepipodophyllotoxin hydrochloride (6). Yield: 5 mg, 0.009 mmol, 38%. White solid. ^{1}H NMR (500 MHz, CD_3OD, 283 K) δ 8.01 (1H, *s*), 6.73 (1H, *s*), 6.68 (1H, *s*), 6.38 (2H, *s*), 6.34 (1H, *br s*), 6.00 (1H, *s*), 5.97 (1H, *s*), 4.79 (1H, *br s*), 4.43 (3H, *br s*), 3.75 (6H, *s*), 3.37 (2H, *br s*), 3.22-3.21 (1H, *m*), 2.91 (6H, *s*). ^{13}C NMR (125 MHz, CD_3OD, 283 K) δ 175.9, 150.7, 149.3, 148.7, 138.2, 136.0, 135.3, 131.2, 128.6, 126.7, 111.4, 109.8, 109.2, 103.4, 69.0, 60.2, 56.7, 52.5, 44.8, 43.2, 42.6, 38.5. HRMS (ESI) *m/z* calcd for $C_{26}H_{29}N_4O_7$ $[M+H]^+$: 509.2031, found: 509.2008.

General procedure for the synthesis of type 2 compounds. 4β-(prop-2-ynyloxy)-4'-demethylepipodophyllotoxin (**4**) or 4β-(prop-2-ynyloxy) epipodophyllotoxin (**5**) (1 equiv) was suspended in a water: *t*-butanol mixture (1:1) and degassed for 5 min with argon. The appropriate azide (10 equiv) was added followed, in order, by sodium ascorbate and $CuSO_4$•$5H_2O$. The mixture was stirred at rt or 50°C till completion. The final suspension was diluted with H_2O and extracted with ethyl acetate. The collected organic phases were dried over $MgSO_4$ and the solvent was removed under reduced pressure. The mixture was purified by flash chromatography or by HPLC.

4β-(1-*N,N*-dimethylaminopropyl-4-methyl-1,2,3-triazolyl)-4'-demethylepipodophyllotoxin hydroformate (7). Yield: 5.5 mg, 0.009 mmol, 26%. White solid. ^{1}H NMR (500 MHz, CD_3OD, 283 K) δ 8.46 (1H, *s*), 8.06 (1H, *s*), 6.93 (1H, *s*), 6.53 (1H, *s*), 6.27 (2H, *s*), 5.98 (1H, *s*), 5.97 (1H, *s*), 4.82-4.73 (3H, *m*), 4.58 (1H, *d*, *J* = 5.0 Hz), 4.54-4.52 (2H, *m*), 4.40-4.37 (1H,

m), 4.33-4.29 (1H, *m*), 3.70 (6H, *s*), 3.40 (1H, *dd*, *J* = 5.0, 14.0 Hz), 3.08-3.04 (2H, *m*), 3.01-2.94 (1H, *m*), 2.80 (6H, *s*), 2.32 (2H, *br s*). ^{13}C NMR (125 MHz, CD_3OD, 283 K) δ 177.5, 169.4, 149.8, 148.5, 148.1, 146.3, 135.6, 134.2, 132.0, 130.7, 125.4, 111.5, 110.8, 109.1, 102.9, 75.2, 69.2, 63.8, 56.6, 56.2, 48.3, 44.9, 43.7, 42.4, 39.7, 26.7. HRMS (ESI) *m/z* calcd for $C_{29}H_{35}N_4O_8$ $[M+H]^+$: 567.2449, found: 567.2457.

4β-(1-(4-hydroxyphenyl)-4-methyl-1,2,3-triazolyl)-4'-demethylepipodophyllotoxin (8). Yield: 8.7 mg, 0.015 mmol, 45%. Grey solid. ^{1}H NMR (600 MHz, $(CD_3)_2SO$, 313 K) δ 8.68 (1H, *s*), 8.21 (1H, *br s*), 7.66 (2H, *d*, *J* = 9.0 Hz), 7.06 (1H, *s*), 6.94 (2H, *d*, *J* = 9.0 Hz), 6.53 (1H, *s*), 6.19 (2H, *s*), 6.03 (1H, *s*), 6.00 (1H, *s*), 4.83-4.75 (3H, *m*), 4.51 (1H, *d*, *J* = 5.0 Hz), 4.39-4.37 (1H, *m*), 4.24-4.21 (1H, *m*), 3.62 (6H, *s*), 3.26 (1H, *br s*), 2.92-2.87 (1H, *m*). ^{13}C NMR (150 MHz, $(CD_3)_2SO$, 313 K) δ 174.4, 157.7, 147.5, 147.1, 146.0, 144.8, 134.7, 132.4, 130.2, 129.5, 128.7, 122.1, 121.8, 115.9, 109.9, 109.6, 108.4, 101.2, 72.9, 67.3, 62.7, 56.0, 42.8, 40.4, 37.7. HRMS (ESI) *m/z* calcd for $C_{30}H_{28}N_3O_9$ $[M+H]^+$: 574.1820, found: 574.1838.

4β-(1-carbomethoxypentyl-4-methyl-1,2,3-triazolyl)-4'-demethylepipodophyllotoxin (9). Yield: 12.9 mg, 0.021 mmol, 62%. White solid. ^{1}H NMR (500 MHz, $CDCl_3$, 283 K) δ 7.55 (1H, *s*), 6.71 (1H, *s*), 6.53 (1H, *s*), 6.24 (2H, *s*), 5.98 (1H, *s*), 5.95 (1H, *s*), 5.43 (1H, *s*), 4.76 (3H, *br s*), 4.60 (1H, *d*, *J* = 5.5 Hz), 4.42-4.35 (2H, *m*), 4.32-4.26 (2H, *m*), 3.76 (6H, *s*), 3.66 (3H, *s*), 3.37 (1H, *dd*, *J* = 5.5, 14.0 Hz), 2.92-2.86 (1H, *m*), 2.32 (2H, *t*, *J* = 7.5 Hz), 1.98-1.92 (2H, *m*), 1.71-1.65 (2H, *m*), 1.38-1.35 (2H, *m*). ^{13}C NMR (125 MHz, $CDCl_3$, 283 K) δ 175.1, 173.8, 148.4, 146.7, 146.2, 144.7, 133.7, 132.5, 130.7, 128.9, 122.6, 110.7, 109.5, 107.5, 101.4, 73.4, 67.4, 63.0, 56.3, 51.6, 50.2, 43.7, 41.1, 38.0, 33.6, 30.0, 25.9, 24.1. HRMS (ESI) *m/z* calcd for $C_{31}H_{36}N_3O_{10}$ $[M+H]^+$: 610.2395, found: 610.2356.

4β-(1-(4-carboxybenzyl)-4-methyl-1,2,3-triazolyl) epipodophyllotoxin (10). Yield: 11.6 mg, 0.018 mmol, 83%. White solid. ^{1}H NMR (500 MHz, $CDCl_3$, 283 K) δ 8.10 (2H, *d*, *J* = 6.0 Hz), 7.52 (1H, *s*), 7.36 (2H, *d*, *J* = 6.0 Hz), 6.69 (1H, *s*), 6.51 (1H, *s*), 6.21 (2H, *s*), 5.98 (1H, *s*), 5.94 (1H, *s*), 5.68-5.58 (2H, *m*), 4.76-4.75 (3H, *m*), 4.58 (1H, *d*, *J* = 5.0 Hz), 4.33-4.25 (2H, *m*), 3.78 (3H, *s*), 3.71 (6H, *s*), 3.36 (1H, *dd*, *J* = 5.0, 14.0 Hz), 2.92-2.86 (1H, *m*). ^{13}C NMR (125 MHz, $CDCl_3$, 283 K) δ 175.0, 170.2, 152.4, 148.4, 146.8, 145.5, 139.9, 136.8, 135.2, 132.4, 131.0, 129.9, 128.7, 127.9, 122.8, 110.7, 109.5, 107.8, 101.5, 73.7, 67.4, 63.0, 60.7, 56.1, 53.8, 43.8, 41.0, 38.0. HRMS (ESI) *m/z* calcd for $C_{33}H_{32}N_3O_{10}$ $[M+H]^+$: 630.2082, found: 630.2097.

ASSOCIATED CONTENT

Supporting information, including detailed synthetic procedures, compound characterization and bioassays, is available free of charge via the Internet at http:// pubs.acs.org.

AUTHOR INFORMATION

Corresponding Author

*raphael.rodriguez@curie.fr; *caroline.austin@ncl.ac.uk

Funding Sources

This research was generously supported by la Fondation pour la Recherche Médicale, La Ligue contre le Cancer, LLR specialist programme 12031 and BCC studentship. R.R. thanks the CNRS for funding.

ACKNOWLEDGMENT

We thank Rodriguez's and Austin's laboratory members for fruitful discussions.

ABBREVIATIONS

TOP2, Topoisomerase II; TOP2A, Topoisomerase IIα; TOP2B, Topoisomerase IIβ; DSBs, double stranded breaks; DDR, DNA-damage response; TARDIS, trapped in agarose DNA immunostaining.

REFERENCES

1. a) Dervan, P. B. Design of sequence-specific DNA-binding molecules. *Science* **1986**, *232*, 464 – 471; b) Gottesfeld, J. M.; Neely, L.; Trauger, J. W.; Baird, E. E.; Dervan, P. B. Regulation of gene expression by small molecules. *Nature* **1997**, *387*, 202 – 205; c) Sun, D.; Thompson, B.; Cathers, B. E. Salazar, M.; Kerwin S. M.; Trent, J. O.; Jenkins, T. C.; Neidle, S. Hurley, L. H. Inhibition of human telomerase by a G-quadruplex-interactive compound. *J. Med. Chem.* **1997**, *40*, 2113 – 2116 ; d) Siddiqui-Jain, A.; Grand, C. L.; Bearss, D. J.; Hurley, L. H. Direct evidence for a G-quadruplex in a promoter region and its targeting with a small molecule to repress c-MYC transcription. *Proc. Natl. Acad. Sci. USA* **2002**, *99*, 11593 – 11598; e) Hurley, L. H. DNA and its associated processes as targets for cancer therapy. *Nat. Rev. Cancer* **2002**, *2*, 188 – 200; f) Neidle, S.; Parkinson, G. Telomere maintenance as a target for anticancer drug discovery. *Nat. Rev. Drug Discov.* **2002**, *1*, 383 – 393; g) Pommier, Y. Topoisomerase I inhibitors: camptothecins and beyond. *Nat. Rev. Cancer* **2006**, *6*, 789 – 802; h) Moorhouse, A. D.; Santos, A. M.; Gunaratnam, M.; Moore, M.; Neidle S.; Moses, J. E. Stabilization of G-quadruplex DNA by highly selective ligands via click chemistry. *J. Am. Chem. Soc.* **2006**, *128*, 15972 – 15973; i) Rodriguez, R.; Müller, S.; Yeoman, J. A.; Trentesaux, C.; Riou, J.-F.; Balasubramanian, S. A novel small molecule that alters shelterin integrity and triggers a DNA-damage response at telomeres**.** *J. Am. Chem. Soc.* **2008**, *130*, 15758 – 15759; j) Rodriguez, R.; Miller, K. M.; Forment, J. V.; Bradshaw, C. R.; Nikan, M.; Britton, S.; Oelschlaegel, T.; Xhemalce, B.; Balasubramanian, S.; Jackson, S. P. Small-molecule–induced DNA damage identifies alternative DNA structures in human genes. *Nat. Chem. Biol.* **2012**, *8*, 301 – 310; k) Wei, D.; Wilson, W. D.; Neidle, S. Small-molecule binding to the DNA minor groove is mediated by a conserved water cluster. *J. Am. Chem. Soc.* **2013**, *135*, 1369 – 1377; l) Rodriguez, R.; Miller, K. M. Unravelling the genomic targets of small molecules using high-throughput sequencing. *Nat. Rev. Genet.* **2014**, *15*, 783 – 796; m) Kang, J. S.; Meier, J. L.; Dervan P. B. Design of sequence-specific DNA binding molecules for DNA me-

thyltransferase inhibition. *J. Am. Chem. Soc.* **2014**, *136*, 3687 – 3694.

2. a) Vos, S. M.; Tretter, E. M.; Schmidt, B. H.; Berger, J. M. All tangled up: how cells direct, manage and exploit topoisomerase function. *Nat. Rev. Mol. Cell Bio.* **2011**, *12*, 827 – 841; b) Chen, S. H.; Chan, N.-L.; Hsieh T. S. New mechanistic and functional insights into DNA topoisomerases. *Annu. Rev. Biochem.* **2013**, *82*, 139 – 170.
3. Bailly, C. Contemporary challenges in the design of topoisomerase II inhibitors for cancer chemotherapy. *Chem. Rev.* **2012**, *112*, 3611 – 3640.
4. a) Nitiss, J. L. Targeting DNA topoisomerase II in cancer chemotherapy. *Nat. Rev. Cancer* **2009**, *9*, 338 – 350; b) Sunter, N. J.; Cowell, I. G.; Willmore, E.; Watters, G. P.; Austin, C. A. Role of topoisomerase IIβ in DNA damage response following IR and Etoposide. *J. Nucleic Acids* **2010**, Article ID 710589, 8 pages.
5. a) Azarova, A. M.; Lyu, Y. L.; Lin, C.-P.; Tsai Y.-C.; Lau, J. Y-N.; Wang, J. C.; Liu L. F. Roles of DNA topoisomerase II isozymes in chemotherapy and secondary malignancies. *Proc. Natl. Acad. Sci. USA*, **2007**, *104*, 11014 – 11019; b) Cowell, I. G.; Sondka, Z.; Smith, K.; Lee, K. C.; Manville, C. M.; Sidorczuk-Lesthuruge, M.; Rance, H. A.; Padget, K.; Jackson, G. H.; Adachi, N.; Austin, C. A. Model for MLL translocations in therapy-related leukemia involving topoisomerase IIβ-mediated DNA strand breaks and gene proximity. *Proc. Natl. Acad. Sci. USA* **2012**, *109,* 8989 – 8994; c) Ezoe, S. Secondary leukemia associated with the anti-cancer agent, etoposide, a topoisomerase II inhibitor. *Int. J. Environ. Res. Public Health* **2012**, *9*, 2444 – 2453; d) Pendleton, M.; Lindsey, R. H.; Felix, C. A.; Grimwade, D.; Osheroff, N. Topoisomerase II and leukemia. *Ann. N. Y. Acad. Sci.* **2014**, *1310*, 98 – 110.
6. Keller-Juslén, C.; Kuhn, M.; Von Wartburg, A. Synthesis and antimitotic activity of glycosidic lignan derivatives related to podophyllotoxin. *J. Med. Chem.* **1971**, *14*, 936 – 940.
7. Willmore, E.; Frank A. J.; Padget, K.; Tilby, M. J.; Austin, C. A. Etoposide targets topoisomerase IIalpha and IIbeta in leukemic cells: isoform-specific cleavable complexes visualized and quantified in situ by a novel immunofluorescence technique. *Mol. Pharmacol.* **1998**, *54*, 78 – 85.
8. Niimi, A.; Suka, N.; Harata, M.; Kikuchi, A.; Mizuno, S. Co-localization of chicken DNA topoisomerase IIα, but not β, with sites of DNA replication and possible involvement of a C-terminal region of α through its binding to PCNA. *Chromosoma* **2001**, *110*, 102–114.
9. a) Ju, B.-G.; Lunyak, V. V.; Perissi, V.; Garcia-Bassets, I.; Rose, D. W.; Glass, C. K.; Rosenfeld, M. G. A topoisomerase IIbeta-mediated dsDNA break required for regulated transcription. *Science* **2006**, *312*, 1798 – 1802; b) Tiwari, V. K.; Burger, L.; Nikoletopoulou, V.; Deogracias, R.; Thakurela, S.; Wirbelauer, c.; Kaut, J.; Terranova, R.; Hoerner, L.; Mielke, C.; Boege, F.; Murr, R.; Peters, A. H.; Barde, Y. A.; Schübeler, D. Target genes of topoisomerase IIβ regulate neuronal survival and are defined by their chromatin state. *Proc. Natl. Acad. Sci. USA* **2012**, *109,* E934 - E943; c) Thakurela, S.; Garding, A.; Jung, J.; Schübeler, D.; Burger, L.; Tiwali, V. K. Gene regulation and priming by topoisomerase IIα in embryonic stem cells. *Nat. Commun*. **2013**, *4*, 2478.
10. Errington, F.; Willmore, E.; Tilby, M. J.; Li. L.; Li, G.; Li. W.; Baguley, B. C.; Austin, C. A. Murine transgenic cells lacking DNA topoisomerase IIbeta are resistant to acridines and mitoxantrone: analysis of cytotoxicity and cleavable complex formation. *Mol. Pharmacol.* **1999**, *56*, 1309 – 1316.
11. Toyoda, E.; Kagaya, S.; Cowell, I. G.; Kurosawa, A.; Kamoshita, K.; Nishikawa, K.; Iizumi, S.; Koyama, H.; Austin, C. A.; Adachi, N. NK314, a topoisomerase II inhibitor that specifically targets the α isoform. *J. Biol. Chem.* **2008**, *283*, 23711 – 23720.
12. Wu, C.-C.; Li, T.-K.; Farh, L.; Lin, L.-Y.; Lin, T.-S.; Yu, Y.-J.; Yen, T.-J.; Chiang, C.-W.; Chan, N.-L. Structural basis of type II topoisomerase inhibition by the anticancer drug etoposide. *Science* **2011**, *333*, 459–462.
13. Cullen, M. E.; Wyke, A. W.; Kuroda, R.; Fisher, L. M. Cloning and characterization of a DNA gyrase A gene from Escherichia coli that confers clinical resistance to 4-quinolones. *Antimicrob. Agents Chemother.* **1989**, *33*, 886 – 894.
14. Cowell, I. G.; Tilby, M. J.; Austin, C. A. An overview of the visualisation and quantitation of low and high MW DNA adducts using the trapped in agarose DNA immunostaining (TARDIS) assay. *Mutagenesis* **2011**, *26*, 253 – 260.
15. Padget, K.; Pearson, A. D. J.; Austin, C. A. Quantitation of DNA topoisomerase IIα and β in human leukaemia cells by immunoblottin. *Leukemia* **2000**, *14*, 1997 – 2005.
16. Bonner, W. M.; Redon, C. E.; Dickey, J. S.; Nakamura, A. J.; Sedelnikova, O. A.; Solier, S.; Pommier, Y. GammaH2AX and cancer. *Nat. Rev. Cancer* **2008**, *8*, 957 – 967.
17. a) Huc, I.; Lehn, J.-M. Virtual combinatorial libraries: Dynamic generation of molecular and supramolecular diversity by self-assembly. *Proc. Natl. Acad. Sci. USA* **1997**, *94*, 2106 – 2110; b) Krasiński, A.; Radić, Z.; Manetsch, R.; Raushel, J.; Taylor, P.; Sharpless, K. B.; Kolb, H. C. In situ selection of lead compounds by click chemistry: target-guided optimization of acetylcholinesterase inhibitors. *J. Am. Chem. Soc.* **2005**, *127*, 6686 – 6692; c) Moses, J. E.; Moorhouse, A. D. The growing applications of click chemistry. *Chem. Rev. Soc.*, **2007**, *36*, 1249 – 1262; d) Di Antonio, M.; Biffi, G.; Mariani, A.; Raiber, E.-A.; Rodriguez, R.; Balasubramanian, S. Selective RNA versus DNA G-quadruplex targeting by in situ click chemistry. *Angew. Chem. Int. Ed.* **2012**, *51*, 11073 – 11078.
18. a) Zhou, X.-M.; Wang, Z.-Q.; Chang, J.-Y.; Chen, H.-X.; Cheng, Y.-C.; Lee, K.-H. Antitumor agents. 120. New 4-substituted benzylamine and benzyl ether derivatives of 4'-O-demethylepipodophyllotoxin as potent inhibitors of human DNA topoisomerase II. *J. Med. Chem.* **1991**, *34*, 3346 – 3350; b) Kamal, A.; Laxman, N.; Ramesh, G. Facile and efficient one-pot synthesis of 4β-arylaminopodophyllotoxins: synthesis of DNA topoisomerase II inhibitors (NPF and W-68). *Bioorg. Med. Chem. Lett.* **2000**, *10*, 2059 – 2062.

Table of Contents graphic:

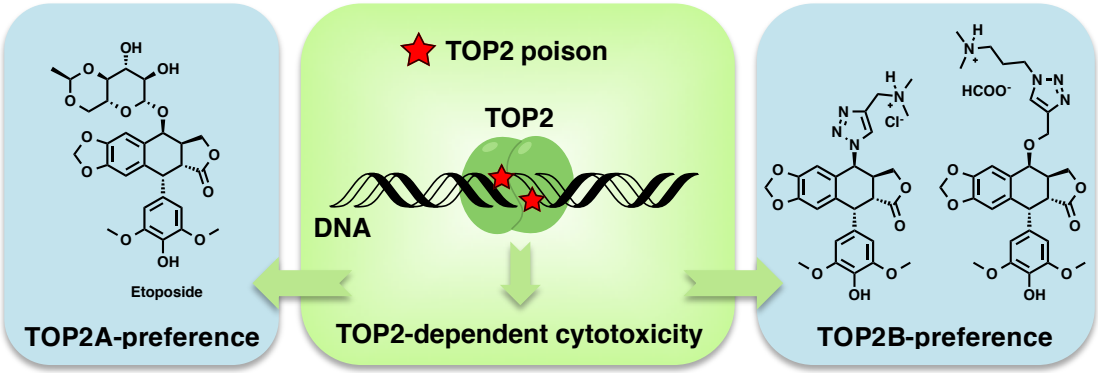

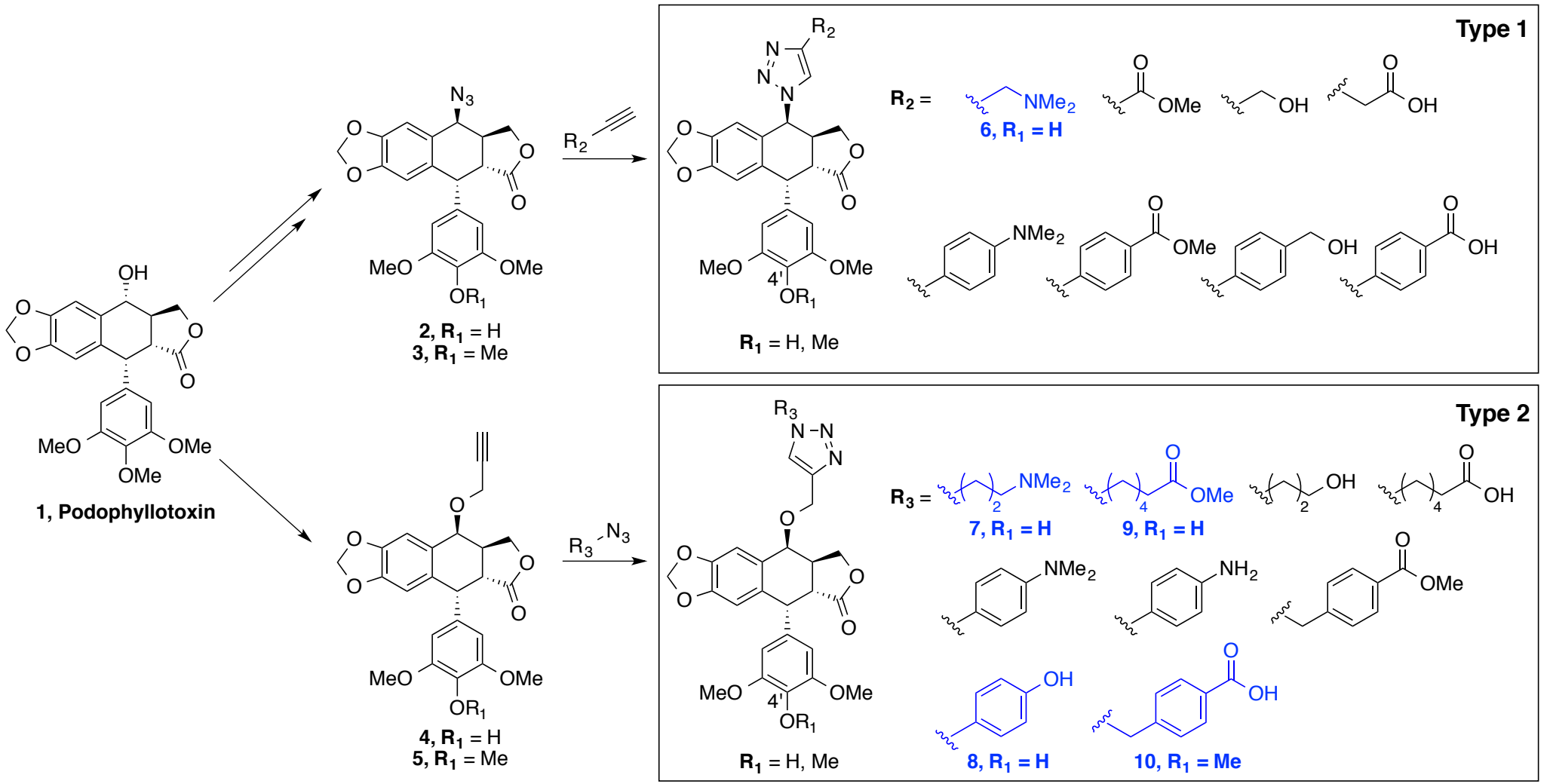
1, Podophyllotoxin
2, R1 = H
3, R1 = Me
4, R1 = H
5, R1 = Me
R1 = H, Me
R1 = H, Me
Type 1
Type 2
R2 =
R3 =
6, R1 = H
7, R1 = H
8, R1 = H
9, R1 = H
10, R1 = Me

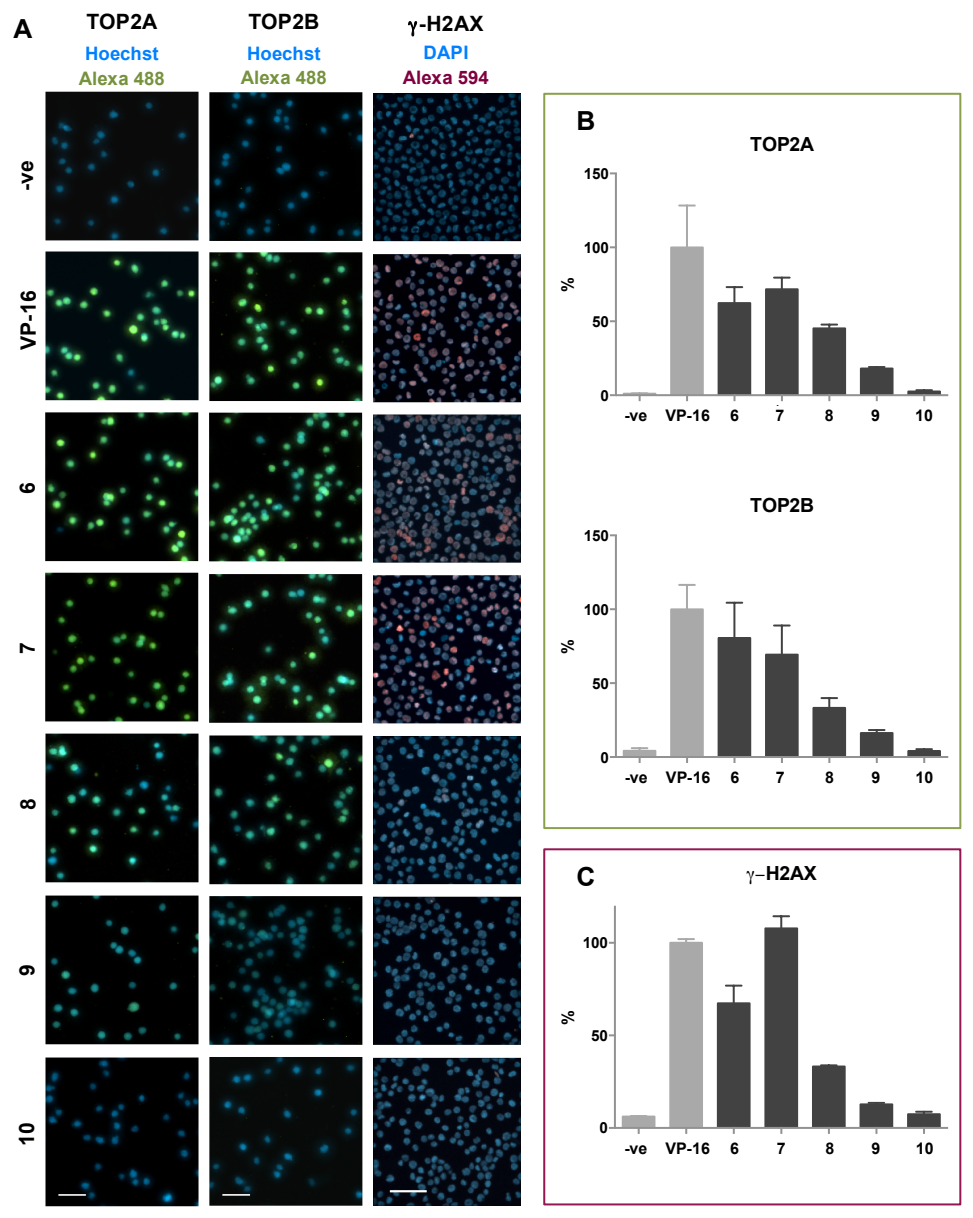
A
TOP2A
Hoechst
Alexa 488
TOP2B
Hoechst
Alexa 488
γ-H2AX
DAPI
Alexa 594
-ve
VP-16
6
7
8
9
10
B
TOP2A
%
150
100
50
0
-ve
VP-16
6
7
8
9
10
TOP2B
%
150
100
50
0
-ve
VP-16
6
7
8
9
10
C
γ–H2AX
%
100
50
0
-ve
VP-16
6
7
8
9
10